

Adsorption and Electronic States of Benzene on Ordered MgO and Al<sub>2</sub>O<sub>3</sub> Thin FilmsS. C. Street, Q. Guo,<sup>†</sup> C. Xu, and D. W. Goodman\*

Department of Chemistry, Texas A&amp;M University, College Station, Texas 77843-3255

Received: June 4, 1996; In Final Form: August 20, 1996<sup>⊗</sup>

The adsorption and electronic structure of benzene (C<sub>6</sub>H<sub>6</sub>) on thin film MgO(100)/Mo(100) and highly ordered Al<sub>2</sub>O<sub>3</sub>/Mo(110) substrates have been studied using temperature-programmed desorption (TPD) and high-resolution electron energy loss spectroscopy (HREELS). Three desorption states have been found for both surfaces. The first corresponds to adsorption of the aromatic ring plane parallel to the surface at low coverages ( $\leq 1$  ML). Intermediate coverages ( $> 1$  ML) give rise to a desorption at a slightly lower temperature, corresponding to the metastable, upright (end-on) adsorption of benzene on the monolayer-covered surface. Large exposures of benzene yield the multilayer with an anomalous higher temperature desorption sequence in the TPD. Both surfaces reveal spectroscopic windows by HREELS between the phonon modes and optical band gap transitions which allow identification of benzene electronic and vibronic transitions. This window is between 2.5 and 5.5 eV in MgO/Mo(100) and 2.5 and 6.7 eV in Al<sub>2</sub>O<sub>3</sub>/Mo(110). Even very low coverages of benzene on these surfaces show the singlet-to-singlet  $^1E_{1u} \leftarrow ^1A_{1g}$  transition. Higher coverages show the loss peaks assigned to  $^3B_{1u} \leftarrow ^1A_{1g}$ ,  $^1B_{2u} \leftarrow ^1A_{1g}$ , and  $^1B_{1u} \leftarrow ^1A_{1g}$  as well. Vibronic bands with  $110 \pm 2$  meV spacing in the loss region of 3.5–5.7 eV are observed. Diminishing vibronic band intensity and loss energy shifts at the lower coverages of benzene as well as TPD results indicate a weak interaction between benzene and Al<sub>2</sub>O<sub>3</sub>/Mo(110) or MgO/Mo(100). The influence of either substrate on the electronic transitions of benzene is weak with respect to the interaction of benzene with metal surfaces, e.g. Ag(111), even though TPD results show similar desorption temperatures.

## 1. Introduction

The adsorption of benzene (C<sub>6</sub>H<sub>6</sub>) on metal single crystal surfaces has received considerable attention, including studies of the adsorption states, the symmetries of adsorbed benzene, the adsorption geometry, and the electronic structure.<sup>1–11</sup> Temperature-programmed desorption (TPD), high-resolution electron energy loss spectroscopy (HREELS), and photoemission studies indicate that benzene chemisorbs molecularly on transition metal single crystal surfaces with the molecular plane parallel to the metal surface upon initial exposure.<sup>1–11</sup>

In studying the interaction between an adsorbate and a surface, the nature of the adsorbate itself is obviously important. A number of spectroscopic methods such as electron impact spectroscopy, extinction coefficient spectroscopy, vacuum-ultraviolet adsorption spectroscopy, ultraviolet photoelectron spectroscopy, and vacuum-ultraviolet resonance Raman spectroscopy have been used to study the electronic structure of benzene.<sup>12–18</sup> A theoretical calculation of the electronic state of benzene has also been carried out.<sup>19</sup> However, these studies have focused on the gas phase, whereas data on the adsorption of benzene on oxide surfaces<sup>20</sup> including semiconducting ZnO<sup>21</sup> or the electronic structure of solid benzene<sup>22</sup> are limited. Because of the differing bonding characteristics of the  $\pi$ - and  $\sigma$ -system, the adsorption behavior of benzene should depend on the orientation of the molecule with respect to the surface.

The study of oxides, most of which are good insulators, by charge particle probes like electrons is hampered by the well-known surface charging problem. To overcome this difficulty, thin oxide films on metal substrates have been successfully prepared in recent years in our laboratory.<sup>23–25</sup> MgO(100) and Al<sub>2</sub>O<sub>3</sub> can be grown epitaxially on a suitable metal substrate.

Also, each has a large optical band gap, allowing the electronic and vibronic transitions of an adsorbate like benzene to be measured.

## 2. Experimental Section

The experiments were carried out in an ultrahigh-vacuum (UHV) chamber with a base pressure of  $2 \times 10^{-10}$  Torr. Briefly, the chamber was equipped with a single-pass cylindrical mirror analyzer (CMA) for Auger electron spectroscopy (AES), reverse view optics for low-energy electron diffraction (LEED), a Model LK-2000 HREEL spectrometer for electron energy loss study, and an UTI quadrupole mass spectrometer (QMS) for temperature-programmed desorption (TPD) measurements.

The Mo(100) and Mo(110) crystal samples were mounted on a probe by spot-welding across two tantalum wires attached to a liquid N<sub>2</sub> cooling reservoir, which allowed cooling to 90 K. The substrate could be resistively heated to 1500 K or heated to 2200 K by electron beam bombardment from the backside of the sample. A W–5% Re/W–26% Re thermocouple was spot-welded to the edge of the crystal for temperature measurements.

The metal surfaces were prepared by annealing in  $2 \times 10^{-8}$  Torr of O<sub>2</sub> at 1200 K with subsequent heating to 2000 K. After several treatments LEED showed very sharp and bright patterns indicative of the  $\langle 100 \rangle$  or  $\langle 110 \rangle$  surfaces. No impurities, such as carbon, were detected by AES except for a very small amount of oxygen. Since both MgO and Al<sub>2</sub>O<sub>3</sub> are subsequently grown on the Mo surfaces in ambient oxygen, the residual oxygen on the surface has no significant influence on the preparation of the thin oxide films.

The MgO and Al<sub>2</sub>O<sub>3</sub> films were prepared using the procedures described previously (refs 25, 27 and 28, respectively). The LEED structure of the as-synthesized Al<sub>2</sub>O<sub>3</sub> ultrathin film reveals only the ordering of the O<sup>2-</sup> anions; there is no evidence regarding ordering of the Al<sup>3+</sup> cations. Since both bulk forms

\* To whom correspondence should be addressed.

<sup>†</sup> Current address: Department of Chemistry, University of Copenhagen, Universitetsparken 5, DK-2100, Copenhagen, Denmark.<sup>⊗</sup> Abstract published in *Advance ACS Abstracts*, October 15, 1996.

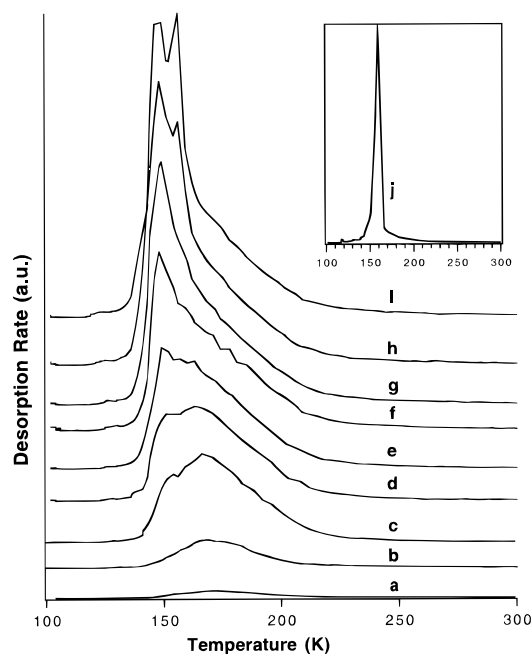


**Figure 1.** Thermal desorption spectra of benzene ( $C_6H_6$ ) from a 20 ML  $MgO(100)/Mo(100)$  surface as a function of increasing exposure at 90 K: (a) 0.0075, (b) 0.015, (c) 0.020, (d) 0.025, (e) 0.030, (f) 0.040, (g) 0.045, (h) 0.050, (i) 0.060, and (j, inset) 0.30 langmuir. Heating rates were 5 K/s.

of alumina—the cubic spinel  $\gamma-Al_2O_3$  and rhombohedral  $\alpha-Al_2O_3$ —have close-packed  $O^{2-}$  planes, definitive surface structure determination in terms of the bulk structures cannot be made from the LEED data alone. The observed hexagonal pattern can be interpreted as arising from either the (111) face of  $\gamma-Al_2O_3$  or the (0001) face of  $\alpha-Al_2O_3$ . Chemically, the as-synthesized alumina film is inert to a variety of probe molecules, indicating the absence of dangling or unsaturated surface bonds.

Spectroscopic grade benzene (>99.0%) was used without further purification. Exposures were determined via an ion gauge without correction for sensitivity. Pressures between  $5 \times 10^{-10}$  and  $1 \times 10^{-9}$  Torr were used during benzene exposure. In TPD experiments the heating rate of 5 K/S was obtained using a computer-controlled temperature ramp. Masses 51, 52, and 78 amu were recorded for the benzene desorption studies. For HREELS, incident energies,  $E_p$ , of 4–25 eV with a typical resolution of 8–24 meV ( $65-194\text{ cm}^{-1}$ ) at full width at half-maximum (fwhm) in the elastic peak were used.

### 3. Results and Discussion

**3.1. Adsorption of Benzene.** A 20-monolayer (ML)  $MgO$  film was prepared on the  $Mo(100)$  surface as described above prior to benzene adsorption. Figure 1 shows the thermal desorption spectra of increasing coverages of benzene from the  $MgO(100)/Mo(100)$  surface following exposure at 90 K. At lower coverages a desorption peak was found at 175 K (Figure 1, curves a and b). Increasing coverage of benzene leads to a second desorption peak at 148 K, as shown in Figure 1 (curves c–g). At higher coverages a third desorption feature appears at 157 K (curves h and i); upon increasing the exposure still further, only one desorption peak is seen at 158 K (Figure 1, insert). A similar desorption sequence for benzene—highest temperature feature present at low coverages, followed by a lower temperature peak and ultimately a single higher temperature feature—is seen in the TPD spectra of benzene on  $Al_2O_3/Mo(110)$  (Figure 2). However, on the alumina surface the temperature range over which the benzene desorbs is much

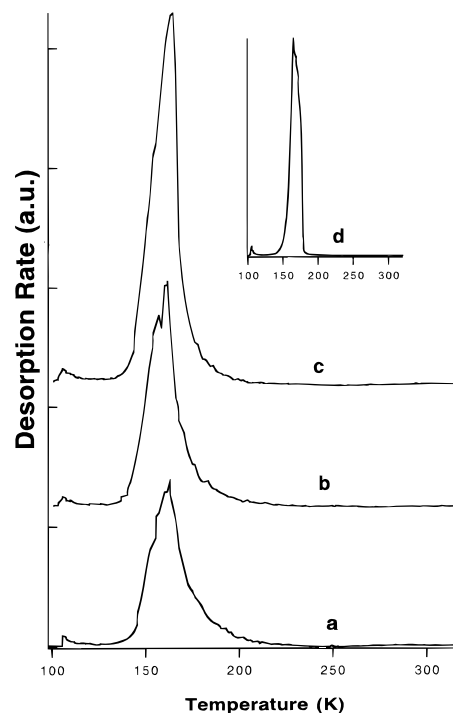


**Figure 2.** Thermal desorption spectra of benzene ( $C_6H_6$ ) from  $\sim 20$  ML  $Al_2O_3(111)/MgO(110)$  surface as a function of increasing exposure at 90 K: (a) 0.020, (b) 0.030, (c) 0.045, and (d, inset) 0.20 langmuir. Heating rates were 5 K/s.

narrower, and the peak desorption temperature at low coverages is lower. At the very low coverages the highest peak desorption temperature is 163 K whereas with increased benzene exposure a feature of 156 K is observed. Multilayer desorption occurs at 164 K.

This anomalous desorption was originally found for benzene desorbing from  $Ru^{1,2}$  and on other metal surfaces, such as  $Ni(110)$ ,<sup>6</sup>  $Ni(100)$ ,<sup>29</sup> and  $Mo(110)$ ,<sup>30</sup> and the identification of a stable bilayer on  $Cu(111)$ .<sup>3</sup> The results of these investigations indicate<sup>1</sup> that the desorption features arise from the geometric arrangement of benzene molecules at the surface as a function of coverage. At coverages up to  $\sim 1.0$  monolayer (1 ML), the molecules chemisorb with their ring planes essentially parallel to the surface. A physisorbed layer having molecules also oriented parallel to the surface adsorbs onto this chemisorbed monolayer. Subsequent adsorption occurs in a metastable state with the molecules “standing up” in the first adsorbed layer, with their ring planes approximately perpendicular to the surface. The intermediate peak desorption temperature found for higher coverages corresponds to desorption of bulklike, randomly oriented (over the long range<sup>1</sup>) benzene multilayers.

Applying the surface selection rule for electron energy loss spectroscopy, different geometries of the adsorbate can be distinguished by the intensity of the vibrational losses.<sup>10,31</sup> The interpretation may be complicated by the presence of the oxide surface, as opposed to a metal surface, and the relative contributions of dipole active and impact scattering mechanisms to the loss intensity. The surface selection rule based on mirror dipole and mirror charge should be valid since the oxide films are less thick than the typical electron–molecule distance for electron–dipole interaction ( $\sim 60\text{ \AA}$ ).<sup>32,33</sup> The contributions to the loss intensity for  $\nu(CH)$  modes is often difficult to determine, but any change in the relative loss intensities between benzene modes of the randomly oriented multilayer and the monolayer are taken to indicate orientation changes in dipole-active modes. Figures 3 and 4 show HREEL spectra of benzene adsorbed on  $MgO(100)/Mo(100)$ . The coverages chosen for display in

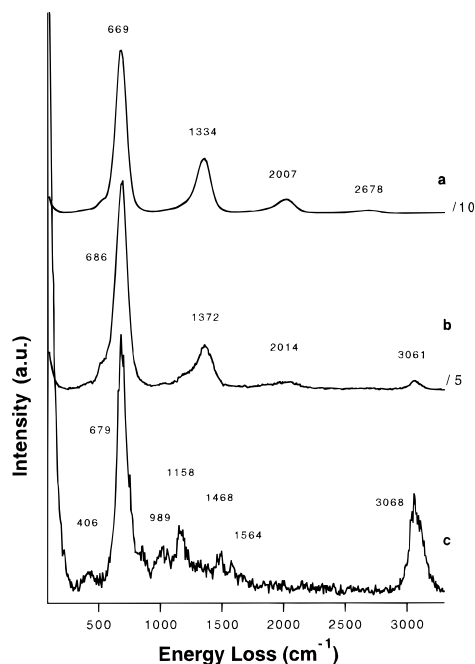


**Figure 3.** HREEL spectra for benzene adsorbed on MgO/Mo(100) as a function of exposure: (a) 0.01, (b) 0.04, and (c) 0.30, langmuir. Primary beam energy was 4.7 eV.

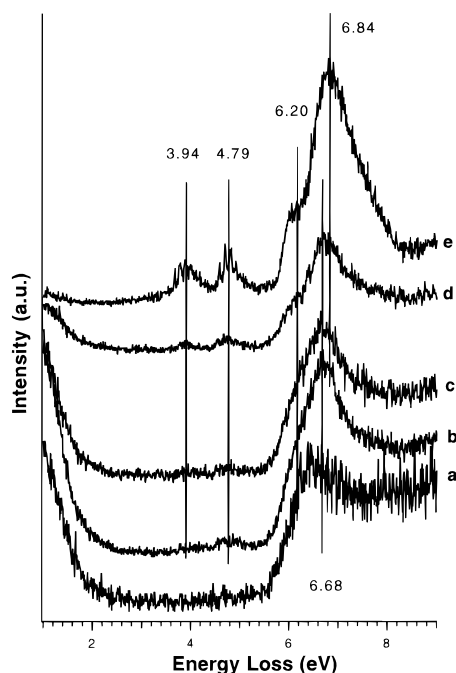


**Figure 4.** Energy loss spectra in the electronic transitions region for benzene adsorbed on MgO/Mo(110) as a function of exposure: (a) clean MgO/Mo(100) substrate; (b) 0.002, (c) 0.005, (d) 0.0075, and (e) 0.30 langmuir. The primary beam energy was 25 eV with 22–24 meV resolution (fwhm) of the elastic peak. The intensity of the elastic peak was  $\sim 3 \times 10^6$ .

Figures 3 and 4 correspond to submonolayer (0.01 langmuir), intermediate second-layer (0.04 langmuir), and multilayer (0.3 langmuir) coverages (1 langmuir =  $1 \times 10^{-6}$  Torr·s). The spectra were collected at 90 K and normalized using the intensity of the elastic peak; the assignments are listed in Table 1. In Figure 3a the losses at 669 and 1334  $\text{cm}^{-1}$  are surface phonon modes of the substrate. For the benzene adsorbed on the MgO-(100)/Mo(100) surface at 0.1 langmuir little change is noted in this loss region, as shown in Figure 3b. With 0.04 langmuir of benzene adsorbed on the surface, losses are found at 686 and

**TABLE 1: Assignment of the Observed Vibrational Frequencies for Multilayer Benzene on the MgO(100) Thin Film at 90 K; Frequencies from Gas Phase Benzene Are Given for Comparison**

mode <sup>a</sup>	vibrational frequency ( $\text{cm}^{-1}$ )	
	multilayer benzene	gas phase <sup>35–37</sup>
$\gamma(\text{CC})$	406	404–410
$\gamma(\text{CH})$	679	673–675
$\gamma(\text{CH})$	841	846–849
$\gamma(\text{CH})$	989	991–992
$\delta(\text{CH})$	1158	1146–1150
$\nu(\text{CC})$	1468	1479–1486
$\nu(\text{CC})$	1564	1595–1596
$\nu(\text{CH})$	3068	3062

<sup>a</sup>  $\gamma$  = out-of-plane bend,  $\delta$  = in-plane, and  $\nu$  = stretch.

1372  $\text{cm}^{-1}$  (Figure 3c). These features are similar in frequency to the phonon modes of the substrate; however, both modes shift slightly while the intensity of the higher frequency mode is significantly reduced (cf. parts c and a of Figure 3). In Figure 3a the features at 2007 and 2678  $\text{cm}^{-1}$  are also due to phonon losses from the substrate. The relative intensity of the peak at 3061  $\text{cm}^{-1}$  increases with increasing benzene exposure (Figure 3b). Comparing the spectra of adsorbed benzene to the spectrum of the clean surface, the losses at 686, 1372, and 3061  $\text{cm}^{-1}$  for 0.04 langmuir benzene coverage are assigned to adsorbed benzene. The HREEL spectrum of multilayer benzene (0.3 langmuir) is shown in Figure 3c. The loss at 679  $\text{cm}^{-1}$  is a dominant dipole-active mode for the benzene film. The in-plane C–H bending mode ( $\gamma_{\text{ip}}(\text{CH})$ ) at 989  $\text{cm}^{-1}$  and C–C ( $\nu(\text{CC})$ ) and C–H ( $\nu(\text{CH})$ ) stretches at 1468 and 3068  $\text{cm}^{-1}$ , respectively, are dipole-active as well. It has been shown that the  $\gamma_{\text{op}}(\text{CH})$  (out-of-plane bending) mode is sensitive to the nature of the adsorption site and the chemisorption bond strength;<sup>5</sup> that is, the larger the deviation in frequency of the  $\gamma_{\text{op}}(\text{CH})$  mode from its gas phase value, the stronger the interaction between benzene and the substrate. For example, the  $\gamma_{\text{op}}(\text{CH})$  frequency in metal–benzene complexes was found to increase in the order  $\text{Ni} < \text{Co} < \text{Fe} < \text{Cr}$ .<sup>34</sup> Where benzene is adsorbed parallel to the surface (0.01 langmuir exposure, low coverage), the  $\gamma_{\text{op}}(\text{CH})$  mode at 679  $\text{cm}^{-1}$  should, and indeed does, have the most significant loss intensity. Unfortunately, at this low exposure it is impossible to distinguish the losses due to adsorbed benzene from the phonon losses of the underlying MgO/Mo(100). The selection rules indicate that the losses at 989, 1468, and 3068  $\text{cm}^{-1}$  should be present for benzene molecules adsorbed in a nonparallel configuration with respect to the surface. The loss frequencies observed agree with those found for benzene gas, indicating formation of randomly oriented multilayers.

The intensity ratio of the losses at 1158, 1468, and 3068  $\text{cm}^{-1}$  to the loss of 679  $\text{cm}^{-1}$  has been used to measure the mean tilt of the benzene plane with respect to the surface.<sup>10,31,35–37</sup> A small intensity ratio indicates parallel orientation of the benzene molecules; the greater the tilt, the larger the intensity ratio. While the interference of the phonon loss at 669  $\text{cm}^{-1}$  makes comparisons involving  $\gamma_{\text{op}}(\text{CH})$  difficult, the very low intensity of the  $\nu_{\text{ip}}(\text{CH})$  (in-plane C–H stretch at 3046  $\text{cm}^{-1}$  in Figure 4b) at low coverage compared to the corresponding losses in the spectra of benzene at higher coverages (Figure 3b,c) indicates that initial benzene adsorption is nondissociative with the benzene molecular plane oriented parallel to the surface. This result is consistent with the TPD results discussed above.

The growth of the benzene film on the MgO/Mo(100) was also studied by LEED. The results show that adsorbed benzene is disordered at 90 K.

**3.2. Electronic States.** The electronic transitions of benzene adsorbed on MgO/Mo(100) and Al<sub>2</sub>O<sub>3</sub>/Mo(110) have been measured by HREELS using a primary beam energy of 25 eV with 20–24 meV resolution (fwhm) of the elastic peak. Figure 4 shows the EEL spectra of the MgO/Mo(100) surface as a function of increasing benzene coverage at 90 K. For a clean MgO film a feature at 6.5 eV is found. This energy is considerably less than the 7.8 eV band gap of bulk MgO<sup>38</sup> and is due to interband transitions associated with surface atoms of 5-fold coordination.<sup>39,40</sup> Figure 4a shows that the surface band gap of the MgO film nevertheless gives a “flat” region between 2.5 and 5.5 eV, which makes convenient the study of adsorbate electronic structure, even at low coverages. A coverage of 0.0025 langmuir of benzene on the MgO(100)/Mo(100) surfaces causes a loss change shown in Figure 4b. The peak at 6.5 eV from the clean substrate shifts to 6.68 eV. A weak feature at ca. 4.7 eV can also be seen. With increasing exposure of benzene the intensity of the loss at 4.7 eV increases, and a new peak at 3.9 eV appears (Figure 4c). A shoulder around 6.2 eV is detected for a 0.0075 langmuir benzene exposure (Figure 4d). At coverages greater than 0.0075 langmuir the relative intensity losses do not change. For multilayer benzene the losses at 3.94, 4.79, 6.20, and 6.84 eV (in Figure 4e) are assigned to  ${}^3B_{1u} \leftarrow {}^1A_{1g}$ ,  ${}^1B_{2u} \leftarrow {}^1A_{1g}$ ,  ${}^1B_{1u} \leftarrow {}^1A_{1g}$ , and  ${}^1E_{1u} \leftarrow {}^1A_{1g}$ , respectively. From both theoretical and experimental studies it is known that the two lower energy optical transitions are the forbidden excitations to  ${}^1B_{2u}$  and  ${}^3B_{1u}$  states caused by vibronic coupling to the allowed  ${}^1E_{1u}$  state (all transitions are  $\pi-\pi^*$ ).<sup>18</sup> The ground state of benzene is totally symmetric ( $A_{1g}$ ). Strict symmetry arguments indicate that the transition  $A_{1g}$  to  $E_{1u}$  is allowed but that the transitions  $A_{1g}$  to  $B_{2u}$  and  $A_{1g}$  to  $B_{1u}$  are forbidden dipole transitions.<sup>41</sup> However, an interaction with molecular vibrations leads to a partial breakdown in the selection rules, resulting in the transitions shown in Figure 4. The most intense peak at 6.84 eV is assigned to the allowed transition to the  ${}^1E_{1u}$  state.

The results of the EEL spectra of benzene on Al<sub>2</sub>O<sub>3</sub>/Mo(110) are very similar. The surface band gap gives a featureless region in the spectrum (Figure 5a) of the clean substrate between 2.5 and 6.7 eV. Again, the apparent surface band gap is significantly lower than the optical bulk band gap transition, which is  $\sim 9.5$  eV. At a benzene coverage of  $\sim 1$  ML, loss features appear as shown in Figure 5b. With increasing benzene exposure the fine structure in the loss modes become more pronounced (Figure 5c), and for multilayer benzene the losses at 3.94, 4.84, 6.19, and 6.86 eV are assigned to  ${}^3B_{1u} \leftarrow {}^1A_{1g}$ ,  ${}^1B_{2u} \leftarrow {}^1A_{1g}$ ,  ${}^1B_{1u} \leftarrow {}^1A_{1g}$ , and  ${}^1E_{1u} \leftarrow {}^1A_{1g}$ , respectively. The differences in the spectra of benzene on the MgO/Mo(100) and Al<sub>2</sub>O<sub>3</sub>/Mo(110) are not significant. Energy differences of  $\sim 0.05$  eV may well be explained by small calibration errors.

At low benzene coverages the intensities of the  ${}^3B_{1u} \leftarrow {}^1A_{1g}$  and  ${}^1B_{2u} \leftarrow {}^1A_{1g}$  transitions are quite weak. The TPD studies indicate that upon initial exposure benzene is oriented with the ring planes parallel to the surface, consistent with the molecule–surface interaction being primarily through the  $\pi$ -system. Thus, the  $\pi-\pi^*$  transitions in the first layer are expected to have decreased intensity with respect to the same transitions in subsequent layers (multilayers). On the MgO(100)/Mo(100) surface the peak positions of the transitions to the  ${}^3B_{1u}$  and  ${}^1B_{2u}$  states are shifted to lower loss energies at low ( $\sim 1$  ML) coverage (Figure 6). This is consistent with significant interaction between benzene and MgO/Mo(100) upon initial adsorption. The position of the transition to  ${}^1E_{1u}$  at 6.84 eV for multilayer benzene is shifted to 6.68 eV (Figure 4) for the case of low coverage and supports the finding of an interaction between

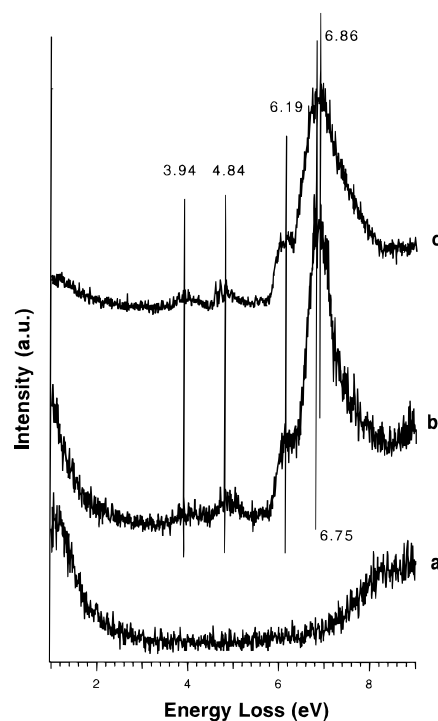


**Figure 5.** Energy loss spectra in the electronic transitions region for benzene adsorbed on Al<sub>2</sub>O<sub>3</sub>/Mo(110) as a function of exposure: (a) clean Al<sub>2</sub>O<sub>3</sub>/Mo(110) substrate; (b) 0.030 and (c) 0.04 langmuir. The primary beam energy was 25 eV with 19–22 meV resolution (fwhm) of the elastic peak. The intensity of the elastic peak was  $\sim 3 \times 10^6$ .

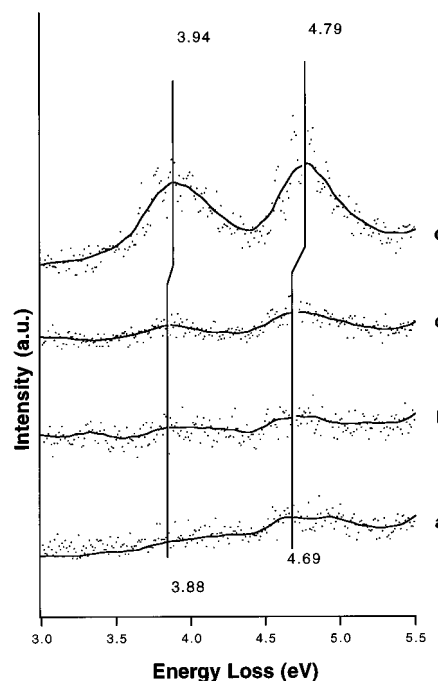


**Figure 6.** Energy shifts of the electronic transitions at low benzene coverage on the MgO/Mo(100) surface. Primary beam energy was 25 eV. The exposures are (a) 0.002, (b) 0.005, (c) 0.0075, and (d) 0.30 langmuir (see Figure 5).

the first adsorbed layer of benzene and the substrate. A similar shift in the energy of the  ${}^1E_{1u}$  transition from very low coverages to multilayer coverages is seen for benzene adsorbed on alumina (Figure 5b,c). The corresponding transition is at 6.86 eV in the multilayer, shifted to 6.75 eV at low coverage. The greater shift in the energy of the  ${}^1E_{1u}$  and  ${}^1B_{2u}$  transitions on magnesia compared to alumina indicates a slightly greater influence of the magnesia on the adsorbed benzene. This is in accord with

**TABLE 2: Energy (eV) of Electronic Transitions from the Benzene Film on the MgO/Mo(100), Al<sub>2</sub>O<sub>3</sub>/Mo(110), and Ag(111)<sup>44</sup> Surfaces; Energy of Benzene Gas Phase Transitions, from Various Sources, Is Also Given**

state	MgO/ Mo(100)	Al <sub>2</sub> O <sub>3</sub> / Mo(110)	Ag(111) <sup>44</sup>	gas phase			
				ref 12	ref 13	ref 14	ref 15
<sup>1</sup> E <sub>1u</sub>	6.84	6.86	7.0	6.95	6.95	6.95	6.95
<sup>1</sup> B <sub>1u</sub>	6.20	6.19	6.35	6.2	6.20	6.25	
<sup>1</sup> B <sub>2u</sub>	4.79	4.84	(4.95) <sup>a</sup>	5.0	4.89	4.80	4.89
<sup>3</sup> B <sub>1u</sub>	3.94	3.94		3.9	3.89	3.90	3.89

<sup>a</sup> This transition is identified as <sup>3</sup>E<sub>1u</sub> ← <sup>1</sup>A<sub>1g</sub> in ref 44. The corresponding transition in the gas phase references is at 4.85 eV (very close to the listed 4.89 eV for the <sup>1</sup>B<sub>2u</sub> transition<sup>15</sup>). In either case the transition energy is higher for benzene adsorbed on the metal than in the gas phase or adsorbed on the oxide thin films.

the desorption results which show that benzene desorbs at a slightly higher temperature on magnesia than on alumina.

Significant energy loss shifts are found for the spectra of benzene adsorbed on the oxide surfaces compared to benzene in the gas phase. We have compared our data with that found for gas phase and condensed benzene, for which the electronic energy levels and electron impact spectroscopy have been studied, refs 12–16 and 1–11, respectively. The highest occupied molecular orbitals in benzene have the symmetries e<sub>1g</sub> (π<sub>2</sub>, π<sub>3</sub>), e<sub>2g</sub> (σ), and o<sub>2u</sub> (π<sub>1</sub>). The energy losses from singlet–singlet transitions caused by excitation of an e<sub>1g</sub> electron to an o<sub>2u</sub> (π\*) orbital have been determined.<sup>12,14,15,36</sup> Table 2 gives the assignments of the transition energies in our experiments as well as the values of the electronic transitions for gas phase benzene from the literature. The transition energies are somewhat smaller in the solid than the gas phase because of the enhanced molecule–molecule interaction. It has been pointed out, for instance, that the value for the <sup>1</sup>B<sub>2u</sub> ← <sup>1</sup>A<sub>1g</sub> transition in a pure benzene crystal should be 0.027 eV lower than the same transition in the gas phase.<sup>42</sup> The influence of magnesia on the loss energies is greater than that. Table 2 shows that our results agree well with the gas phase data, with a difference in the loss energy which reflects a perturbation in the energy of the <sup>1</sup>B<sub>2u</sub> ← <sup>1</sup>A<sub>1g</sub> transition due to adsorbate–surface interactions. For multilayer benzene the electronic transition data have been collected with different incident angles, and the relative intensity ratios of the transition losses are the same, indicating that the multilayer benzene film consists of randomly oriented molecules.

The influence noted above is made more apparent in the results obtained in our ELS study with respect to the vibronic band structure in the benzene film. Figures 7 and 8 show the band structure for multilayer coverages of benzene on the MgO/Mo(100) and Al<sub>2</sub>O<sub>3</sub>/Mo(110) surfaces, respectively, in the region of the <sup>3</sup>B<sub>1u</sub> and <sup>1</sup>B<sub>2u</sub> transitions. (This fine structure is also apparent, but less well-defined, at lower coverages as shown in Figures 4 and 5.) The spacing between the bands in both transitions is 110 ± 2 meV, which is in good agreement with the value of 115 meV for the coupling with the ground state of the symmetric ring “breathing” vibration in the gas phase.<sup>7</sup> For the species adsorbed on a surface, this spacing probably reflects the ground state out-of-plane CH bending modes. (In any event the vibrations of the molecule are likely to be highly coupled.) Other vibronic bands are observed at ~5.5 and ~5.6 eV as shown in Figures 7 and 8. In the gas phase these peaks were found to be singlet–triplet transitions.<sup>12,43</sup> The band structure assignments and comparison to the gas phase are given in Table 3.

Spectra of the benzene film obtained on a surface using HREELS are of better quality, in terms of resolution and signal-

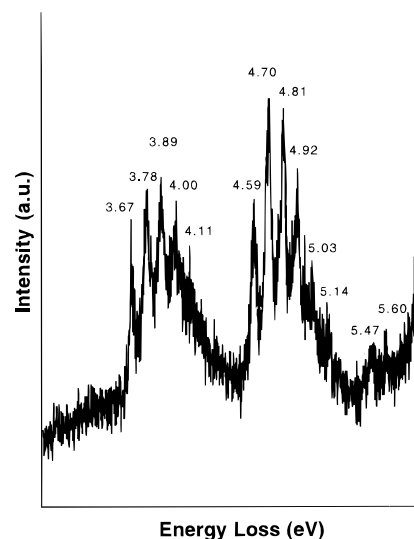


**Figure 7.** Energy loss spectrum of ~1 ML benzene on the MgO/Mo(100) surface showing the vibronic fine structure. Benzene exposure was 0.030 langmuir. The primary beam energy was 25 eV with 22 meV resolution (fwhm) of the elastic peak.

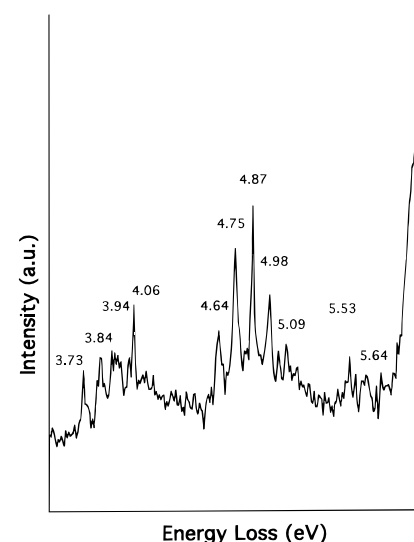


**Figure 8.** Energy loss spectrum of ~1 ML benzene on the Al<sub>2</sub>O<sub>3</sub>/Mo(110) surface showing the vibronic fine structure. Benzene exposure was 0.030 langmuir. The primary beam energy was 25 eV with 19 meV resolution (fwhm) of the elastic peak.

**TABLE 3: Comparison of the Energies of Vibronic Transitions in Adsorbed Benzene by HREELS with Gas-Phase Electron Impact Data**

state	MgO/Mo(100)	Al <sub>2</sub> O <sub>3</sub> /Mo(110)	gas phase <sup>15</sup>
<sup>3</sup> B <sub>2u</sub>	5.60	5.64	5.69
	5.47	5.53	5.58
	5.03	5.09	5.11
<sup>1</sup> B <sub>2u</sub>	4.92	4.98	5.01
	4.81	4.87	4.89
	4.70	4.75	4.78
	4.59 <sup>a</sup>	4.64 <sup>a</sup>	(4.65) <sup>a,b</sup>
<sup>3</sup> B <sub>1u</sub>	4.00	4.06	3.98
	3.89	3.94	3.89
	3.78	3.84	3.79
	3.67	3.73	3.67 sh

<sup>a</sup> This transition has also been assigned to <sup>3</sup>E<sub>1u</sub> ← <sup>1</sup>A<sub>1g</sub>.<sup>15,44</sup> <sup>b</sup> This transition energy was identified in ultraviolet absorption experiments.<sup>15</sup>

to-noise, than the electron impact spectra of gas phase benzene found in the literature. This is probably because of the relatively high concentration on the surface compared to the gas phase. It

should be noted that the intensities of the losses at  $\sim 5.5$  and  $\sim 5.6$  eV in our experiments are very weak compared to the intensities of the same features in the reference spectra. At lower benzene coverages the intensities of these transitions are negligible, and the intensity of the  ${}^3\text{B}_{1u} \leftarrow {}^1\text{A}_{1g}$  transition is considerably reduced (see Figures 4d and 5b), indicating very short lifetimes for these excited states.

The electronic spectra of benzene on the oxide surface can also be compared to the results obtained for benzene adsorption on Ag(111).<sup>44</sup> On Ag(111) the  $\pi-\pi^*$  transitions are shifted to higher energies compared to the gas phase (see Table 2). The loss features are much broader on the metal surface with no apparent vibronic fine structure even though the experimental conditions were quite similar ( $\sim 1-3$  ML of benzene, adsorbed at 140 K or below, ELS spectra using a primary beam energy of 20 meV). On metals, the lifetimes of the excited states are shorter than for the corresponding ones on oxide surfaces. The TPD spectra of benzene from Ag(111) indicate that the molecules are more strongly adsorbed on the metal surface than on the oxide surfaces. In fact, while the multilayer desorption temperature of  $\sim 150$  K<sup>45</sup> is similar to that found for desorption from the oxides, there are real differences in the peak desorption temperature for very low coverages. On metals such as Cu(111)<sup>3</sup> and Ag(111),<sup>44</sup> the desorption temperatures at very low coverages of benzene are ca. 220 K. A similarly strong initial layer interaction was found for benzene adsorption on ZnO(1010) (peak temperature of desorption ca. 250 K<sup>21</sup>). These peak desorption temperatures are a sensitive measure of the interaction of the benzene ring with the surface, suggesting that the relative strength of the interaction is  $\text{Cu} \approx \text{Ag} > \text{MgO} > \text{Al}_2\text{O}_3$ . Nevertheless, benzene on silver or copper and on alumina or magnesia are similar in that the benzene ring is only weakly interacting with the surface ( $\Delta H_{\text{ads}} = 10-13$  kcal/mol). Substantial symmetry reduction is found for benzene on Ag(111), resulting in an apparent perturbation of the highest occupied molecular orbital (HOMO).<sup>45</sup> Classic image field theory was not sufficient to explain the observed energy shifts in the electronic transitions on Ag(111),<sup>44</sup> but it appears that the weak interaction of the benzene molecular  $\pi$ -system with the metal d-orbitals stabilizes the ground state  $\pi$ -orbitals by several tenths of an electronvolt,<sup>45,46</sup> increasing the transition energies. This is obviously not the case for benzene on the insulating metal oxides. The  $\pi$ -system appears to interact with the filled O(2p) band of the oxygen-terminated oxide surface,<sup>25</sup> leading to the destabilization which slightly decreases the energy of the  $\pi-\pi^*$  transitions. It is noteworthy that the vibronic fine structure, which is seen for the relatively long-lived electronic transitions of benzene on the oxide surfaces, is not found on metal surfaces because the screening effects of the metal shortens the lifetime of the excited state, broadening the corresponding loss feature. This is consistent with a stronger interaction of the benzene  $\pi$ -system with metal surfaces than the oxide surfaces, also indicated by the higher peak temperature of desorption of submonolayer benzene from metal surfaces. The vibronic bands become fairly distinguishable at  $\sim 1$  ML coverage (see Figures 4d, 5b, and 6c). It can be argued, however, that the vibronic resolution arises as a function of the growth of the physisorbed layer which is perhaps somewhat decoupled from  $\pi$ -interaction with the surface by an intervening chemisorbed layer<sup>1</sup> (see section 3.1). This is the second time that vibronic fine structure of a (sub)monolayer adsorbate has been identified, and the results presented here support the conclusions of Freund and co-workers as to the lifetimes of electronically excited states of molecules on oxide versus metal surfaces.<sup>47</sup>

#### 4. Conclusion

We have studied the adsorption of benzene on ordered thin films of MgO and  $\text{Al}_2\text{O}_3$  grown on Mo single crystal substrates by TPD and HREELS. Three thermal desorption states are identified on both substrates. At very low coverages ( $\leq 1$  ML) a high-temperature desorption feature is associated with adsorption of the benzene plane parallel to the surface. With increasing coverage a metastable, low-temperature desorption state indicates upright (end-on) adsorption of the molecules to the underlying monolayer. At higher coverages a single desorption feature is associated with the multilayer. The low temperatures of these desorption states for both substrates (150–175 K) indicate weak interactions between benzene and the oxide thin films ( $\sim 10-12$  kcal/mol). The TPD data are very similar to previous results for benzene desorption from noble metals,<sup>3,44</sup> which also indicate weakly adsorbed benzene with very similar multilayer desorption temperatures as a function of coverage. The differences between the metals and the metal oxides are in the temperatures of desorption of the low coverage ( $\sim 1$  ML) states, indicating stronger interaction of the benzene  $\pi$ -system with the metal d-orbitals than with the metal oxides.

The electronic spectra of benzene adsorbed on alumina and magnesia show the allowed transition from the ground state to  ${}^1\text{E}_{1u}$  as well as the weaker "forbidden" transitions to  ${}^3\text{B}_{1u}$ ,  ${}^1\text{B}_{2u}$ , and  ${}^1\text{B}_{1u}$ , present because of symmetry-breaking vibronic interactions. Approaching multilayer coverages the vibronic fine structure bands with 110 meV spacing are observed. The energies of the observed transitions are only slightly less than their counterparts for benzene in the gas phase, which indicates a weak interaction between the molecular  $\pi$ -system and the oxide substrate, in accord with the TPD results. These results differ from the ELS spectra of benzene on Ag(111),<sup>44</sup> where it was found that interaction with the metal d-orbitals shifted the benzene  $\pi-\pi^*$  transitions to slightly higher energies. The transitions on metals surfaces were also significantly broader, with no observable fine vibronic structure, indicating short excited lifetimes and a stronger interaction than found for the weakly interacting magnesia and alumina surfaces.

**Acknowledgment.** We acknowledge with pleasure the support of this work by the National Science Foundation under Contract DMR 9423707. We express our sadness at the passing of Prof. Brian E. Bent. The loss of him is a loss not only to his many friends and colleagues but to surface science and the scientific community as a whole.

#### References and Notes

- (1) Jakob, P.; Menzel, D. *Surf. Sci.* **1989**, 220, 70.
- (2) Polat, J. A.; Thiel, P. A. *J. Am. Chem. Soc.* **1986**, 108, 7560.
- (3) Xi, M.; Yang, M. X.; Jo, S. K.; Bent, B. E. *J. Chem. Phys.* **1994**, 101, 9122.
- (4) Nishijima, M.; Fujisawa, M.; Takaoka, T.; Sekitani, T. *Surf. Sci.* **1993**, 283, 121.
- (5) Koel, B. E.; Crowell, J. E.; Mate, C. M.; Somorjai, G. A. *J. Phys. Chem.* **1984**, 88, 1988.
- (6) Huntley, D. R.; Jordan, S. L.; Grimm, F. A. *J. Phys. Chem.* **1992**, 96, 1409.
- (7) Jakob, P.; Menzel, D. *Surf. Sci.* **1988**, 201, 503.
- (8) Taguchi, Y.; Fujisawa, M.; Nishijima, M. *Chem. Phys. Lett.* **1991**, 178, 363.
- (9) Aarts, J. F. M.; Sassen, N. R. M. *Surf. Sci.* **1989**, 214, 257.
- (10) Lehwald, S.; Ibach, H.; Demuth, J. E. *Surf. Sci.* **1978**, 78, 577.
- (11) Bertolini, J. C.; Rousseau, J. *Surf. Sci.* **1979**, 89, 467.
- (12) Doering, J. P. *J. Chem. Phys.* **1969**, 51, 2866.
- (13) Frueholz, R. P.; Flicker, W. M.; Mosher, O. A.; Kuppermann, A. *J. Chem. Phys.* **1979**, 70, 3057.
- (14) Lessettre, E. N.; Skerbele, A.; Dillon, M.; Ross, K. *J. Chem. Phys.* **1968**, 48, 5066.
- (15) Doering, J. P. *J. Chem. Phys.* **1977**, 67, 4065.

- (16) Philis, J.; Bolovinos, A.; Andritsopoulos, G.; Pantos, E.; Tsekeris, P. *J. Phys. B: At. Mol. Phys.* **1981**, *14*, 3621.
- (17) Amirav, A.; Jortner, J. *J. Chem. Phys.* **1985**, *82*, 4378.
- (18) Sension, R. J.; Brudzynski, R. J.; Hudson, B. *J. Chem. Phys.* **1991**, *94*, 873.
- (19) Hay, P. J.; Shavitt, I. *J. Chem. Phys.* **1974**, *60*, 2865.
- (20) Rubloff, G. W.; Luth, H.; Grobman, W. D. *Chem. Phys. Lett.* **1976**, *39*, 493.
- (21) Pöss, D.; Ranke, W.; Jacobi, K. *Surf. Sci.* **1981**, *105*, 77.
- (22) Colson, S. D.; Bernstein, E. R. *J. Chem. Phys.* **1965**, *43*, 2661.
- (23) Goodman, D. W. *Chem. Rev.* **1995**, *95*, 523.
- (24) Goodman, D. W. *Surf. Rev. Lett.* **1995**, *2*, 9.
- (25) Guo, Q.; Xu, C.; Goodman, D. W. Manuscript in preparation.
- (26) Henrich, V. E.; Cox, P. A. *The Surface Science of Metal Oxides*; Cambridge University Press: Cambridge, 1994.
- (27) Wu, M.-C.; Corneille, J. S.; Estrada, C. A.; He, J.-W.; Goodman, D. W. *Chem. Phys. Lett.* **1991**, *182*, 472.
- (28) Chen, P. J.; Goodman, D. W. *Surf. Sci.* **1994**, *312*, L767.
- (29) Blass, B. M.; Akhter, S.; White, J. M. *Surf. Sci.* **1987**, *191*, 406.
- (30) Liu, A. C.; Friend, C. M. *J. Chem. Phys.* **1988**, *87*, 4396.
- (31) Richardson, N. V. *Surf. Sci.* **1979**, *87*, 622.
- (32) Ibach, H.; Mills, D. L. *Electron Energy Loss Spectroscopy and Surface Vibrations*; Academic Press: New York, 1982.
- (33) Xu, C.; Goodman, D. W. *J. Chem. Soc., Faraday Trans.* **1995**, *91*, 3709.
- (34) Efner, H. F.; Tevault, D. E.; Fox, W. B.; Smardzowski, R. R. *J. Organomet. Chem.* **1978**, *146*, 45.
- (35) Herzberg, G. *Molecular Spectra and Molecular Structure*; Van Nostrand: New York, 1954; Vol. 2.
- (36) Hollinger, A. B.; Wesh, H. L.; Jammn, K. S. *Can. J. Phys.* **1979**, *57*, 767.
- (37) Shimanouchi, T. *Tables of Molecular Vibrational Frequencies*, US GPO: Washington, DC, 1972; Vol. NSRDS-NBS 39.
- (38) Roessler, D. M.; Walker, W. C. *Phys. Rev.* **1967**, *159*, 733.
- (39) Wu, M.-C.; Truong, C. M.; Goodman, D. W. *Phys. Rev. B* **1992**, *56*, 12688.
- (40) Henrich, V. E.; Dresselhaus, G.; Zeiger, H. J. *Phys. Rev. B* **1980**, *22*, 4764.
- (41) Dodd, R. E. *Chemical Spectroscopy*; Elsevier: Amsterdam, 1962.
- (42) Ibach, H.; Lehwald, S. *J. Vac. Sci. Technol.* **1978**, *15*, 407.
- (43) Nieman, G. C.; Robinson, G. W. *J. Chem. Phys.* **1963**, *39*, 1298.
- (44) Avouris, P.; Demuth, J. E. *J. Chem. Phys.* **1981**, *75*, 4783.
- (45) Dudde, R.; Frank, K.-H.; Koch, E.-E. *Surf. Sci.* **1990**, *225*, 267.
- (46) Anderson, A. B.; McDevitt, M. R.; Urbach, F. L. *Surf. Sci.* **1984**, *146*, 80.
- (47) Jaeger, R. M.; Homann, K.; Kühlenbeck, H.; Freund, H.-J. *Chem. Phys. Lett.* **1993**, *203*, 41.

JP961624N